

Phase Diagram of  $^3\text{He}$ - $^4\text{He}$  Mixture in Aerogel

S. B. Kim, J. Ma,\* and M. H. W. Chan

Department of Physics, Penn State University, University Park, Pennsylvania 16802

(Received 28 June 1993)

When a  $^3\text{He}$ - $^4\text{He}$  mixture is placed inside porous aerogel with an open volume fraction of 0.98, the coexistence region is found to be detached from the superfluid transition line, giving rise to a miscible superfluid mixture at high  $^3\text{He}$  concentration and low temperature with intriguing properties.

PACS numbers: 67.60.-g, 67.40.Kk, 67.40.Yv, 67.70.+n

$^3\text{He}$ - $^4\text{He}$  mixtures are without a doubt among the most fascinating binary fluid mixtures. As shown in Fig. 1, the superfluid transition temperature of the bulk miscible mixture is found to decrease with increasing  $^3\text{He}$  concentration. In the bulk fluid, this “ $\lambda$ ” line terminates at the tricritical point at  $T_{\text{tr}}=0.872$  K and  $X_3=0.669$  [1]. Here  $X_3$  is the (molar)  $^3\text{He}$  concentration, i.e.,  $X_3=N_3/(N_3+N_4)$  with  $N_3$  and  $N_4$  being respectively the number of  $^3\text{He}$  and  $^4\text{He}$  atoms in a mixture. Below  $T_{\text{tr}}$ , the mixture phase separates into coexisting  $^3\text{He}$  and  $^4\text{He}$  rich regions. In the  $T=0$  limit, the  $^4\text{He}$  rich fluid contains about 6.4% of  $^3\text{He}$ . In contrast,  $^4\text{He}$  atoms are completely excluded from the  $^3\text{He}$  rich solution [2].

In this paper we report on the effect of dilute quenched impurities in the form of aerogel on the properties of a  $^3\text{He}$ - $^4\text{He}$  mixture. Silica aerogel is a highly porous glass consisting of a tenuous network of  $\text{SiO}_2$  strands interconnected at random sites. It is made from a sol-gel and hypercritical drying process [3]. Although the silica strands of the aerogel used in this experiment constitute only 2% of the available volume, the effect on the entire  $^3\text{He}$ - $^4\text{He}$

phase diagram is profound. Inside aerogel the superfluid transition line is found to extend down towards  $T=0$  K. The coexistence region is detached from this line, thus removing the tricritical point and opening up a region of miscible superfluid on the  $^3\text{He}$  rich side of the phase diagram.

The aerogel induced phase diagram, also shown in Fig. 1, is inferred from torsional oscillator measurements of the superfluid response of about sixty  $^3\text{He}$ - $^4\text{He}$  samples of different concentrations. The silica aerogel sample was grown inside our cylindrical torsional cell of 0.70 cm in diameter and 0.96 cm in height via a two step gelation process [4]. A major advantage of growing aerogel *in situ* is the elimination of any macroscopic voids and hence bulk fluid mixture in the cell. This same torsional cell was used recently to study the effect of this ultralight aerogel on the nature of the superfluid transition in  $^4\text{He}$  and  $^3\text{He}$ - $^4\text{He}$  mixtures [5].

The torsional oscillator was operated at a resonant frequency near 391 Hz. Measurements were made in a  $^3\text{He}$  and in a dilution refrigerator cryostat with the sample at saturated vapor pressure. Each experimental run started with a pure  $^3\text{He}$  sample; subsequent samples are prepared by successive dilutions of  $^4\text{He}$  to the desired  $X_3$ . In order to limit the amount of fluid outside the cell,  $^3\text{He}$  is removed by dosing out  $^3\text{He}$  rich vapor before  $^4\text{He}$  is added [6]. If there is a substantial amount of mixture outside the cell (e.g., inside the hollow torsion rod and capillary),  $X_3$  inside the aerogel cell will decrease with decreasing temperature when the excess bulk undergoes phase separation. By monitoring the period of the oscillator in the normal fluid region, we were able to limit and determine the excess bulk to be less than 2% for all samples. The concentration of each of the samples after multiple dilution was cross checked with samples made with fresh  $^3\text{He}$  and  $^4\text{He}$  gases and found to be accurate to better than 0.5%.

In Fig. 2, the period  $P$  of the torsional cell is shown for mixtures with  $X_3$  higher than 0.88. In these scans there is a broad maximum in  $P$  near 0.5 K reflecting the maximum in the density of pure  $^3\text{He}$  [7] and evidently also  $^3\text{He}$  rich solutions. There is no sign of superfluidity for mixtures with  $X_3$  equal to and higher than 0.98. A clear superfluid onset signal corresponding to a drop in period associated with decoupling of the superfluid mass is seen

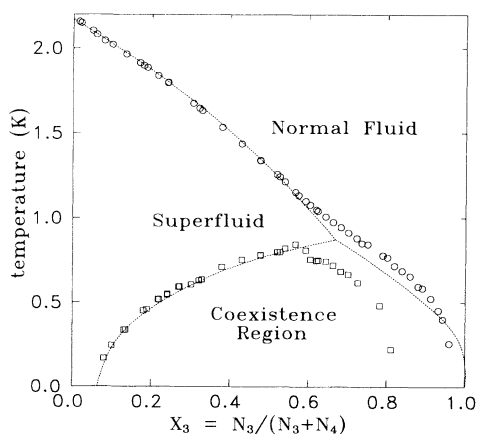


FIG. 1. The phase diagram of  $^3\text{He}$ - $^4\text{He}$  mixture inside aerogel of 0.98 open volume fraction. Circles separate the superfluid and normal fluid regions; squares mark the coexistence region. The detachment of the lambda line from the coexistence boundary opens up a miscible superfluid in the high  $^3\text{He}$  concentration region. The bulk boundaries are shown as dotted lines.

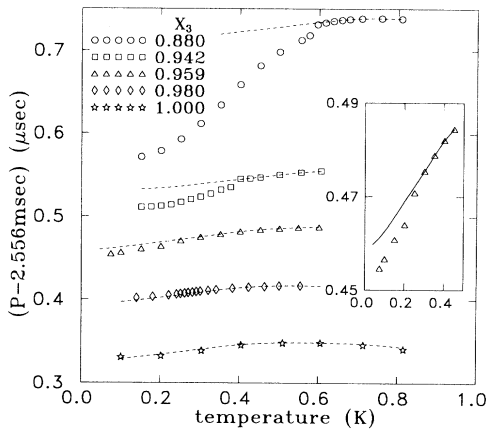


FIG. 2. The period of the oscillator for mixtures with  $X_3 \geq 0.88$ . The period at  $X_3 = 0.88$  has been shifted downward by 60 nsec. The dashed lines show the expected (normal fluid) background extrapolated from the normal fluid region. For pure  $^3\text{He}$ , the temperature dependence of the period is consistent, quantitatively, with that of the density data as determined by Boghosian, Meyer, and Rives [7]. For lack of information, the same temperature dependence is assumed for the background of the mixture samples. Evidence of superfluid onset for the  $X_3 = 0.959$  sample is shown in expanded scale in the inset. The superfluid signals,  $\Delta P$ , or the difference between the measured  $P$  and the background for these mixtures are shown in Fig. 6(a).

at 0.40 K for a mixture with  $X_3 = 0.942$ . A more subtle signal is also seen below 0.26 K for a mixture with  $X_3 = 0.959$ . A smooth extrapolation of the onset temperatures vs  $X_3$  indicate a minimum of  $3.3 \pm 0.2$  at. % of  $^4\text{He}$  (i.e.,  $X_3 = 0.967 \pm 0.002$ ) is required for the observation of superfluidity in the  $T = 0$  K limit.

The superfluid signals,  $\Delta P$ , as a function of temperature for a wide range of  $X_3$  less than 0.7 are shown in Fig. 3.  $\Delta P$  is obtained by subtracting the measured value of  $P$  in the superfluid region at  $T$  from that extrapolated from the normal fluid region. The transition temperature  $T_c$  can be easily picked out from each of these plots and a smooth dependence on  $X_3$  is found (see Fig. 1). For  $X_3$  less than 0.5, the temperature dependence of  $\Delta P$  near  $T_c$  is found to be very similar to that of pure  $^4\text{He}$  [5].

An anomaly is present in each of the  $\Delta P$  vs  $T$  traces shown in Fig. 3 as indicated by the arrows. At temperatures below the anomaly,  $\Delta P$  is found to be dependent on whether measurements were made while cooling or warming. The data shown in Fig. 3 are obtained while warming. In a warming scan, the torsional oscillator cell was first rapidly cooled down from around 1.3 K to the lowest temperature and then warmed up in small successive (i.e., roughly 20 mK) steps. The temperature of the mixing chamber or  $^3\text{He}$  pot was controlled to better than 0.5 mK at each step for typically 2 h, until a time independent period reading was obtained. (Similar 2 h

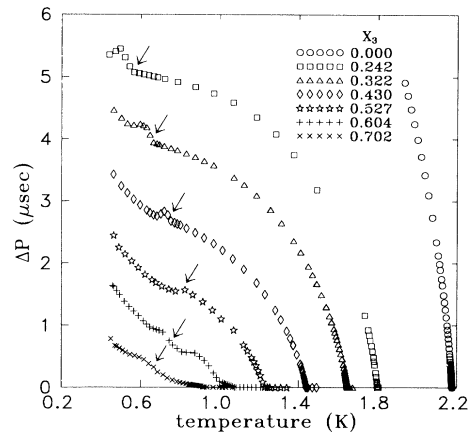


FIG. 3. The superfluid signal ( $\Delta P$ ) for mixtures with  $X_3$  less than 0.7.

waiting periods, to allow for thermal equilibration between the torsional cell and the mixing chamber, were also allotted between each temperature step in the cooling scans.) The history dependent behavior is shown for a number of mixtures in Fig. 4. The value of  $\Delta P$  obtained during warming ( $\Delta P_W$ ) was found to be larger than that during cooling ( $\Delta P_C$ ) for temperatures below a specific, concentration dependent value,  $T_b$ . We have waited for more than 3 d at a temperature  $T < T_b$  during both warming and cooling scans, but  $\Delta P_W$  and  $\Delta P_C$  show no sign of convergence. Data above  $T_b$ , on the other hand, show reproducibility to within 2 nsec. In contrast to samples at lower  $X_3$ , the warming and cooling scans at  $X_3 = 0.839$  displayed in Fig. 4 show no signs of history dependent behavior. This is characteristic of all samples

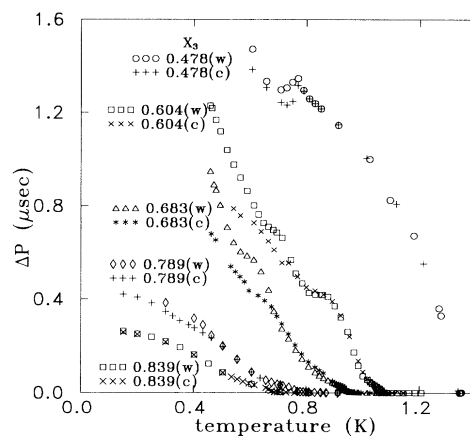


FIG. 4.  $\Delta P$  vs temperature scans for five different mixtures. (W) and (C) indicate, respectively, warming and cooling scans. The value of  $\Delta P$  for  $X_3 = 0.478$  and  $X_3 = 0.604$  samples has been multiplied by 0.6 and 0.75, respectively. History dependent  $\Delta P$  is found below specific (phase separations) temperatures for all mixture samples except that at  $X_3 = 0.839$ .

with  $X_3$  larger than 0.81.

In Fig. 5, the amplitude of the oscillation, which is inversely proportional to dissipation, is shown for a number of samples. With the exception of the scans at  $X_3=0.839$  and  $X_3=0.06$ , each of these scans show a signature (dip or step) in dissipation at  $T_b$ , the onset temperature for history dependent behavior in  $\Delta P$ . The difference between  $\Delta P_W$  and  $\Delta P_C$  below  $T_b$  decreases with  $X_3$  for  $X_3$  less than 0.50. For samples with  $X_3 \lesssim 0.40$ , the difference between  $\Delta P_W$  and  $\Delta P_C$  becomes vanishingly small and undetectable. The signature in dissipation, however, persists down to at least  $X_3=0.080$ . We interpret the signature in dissipation at  $T_b$  as evidence of the mixture undergoing phase separation into  $^3\text{He}$  and  $^4\text{He}$  rich regions. Since the zero point energy of  $^4\text{He}$  is smaller than that of  $^3\text{He}$ , the  $^4\text{He}$  rich phase is expected to reside on the average closer to the silica strands to maximize the benefit from van der Waals interactions. When the mixture is cooled into the coexistence region, the interface separating the two fluids will be quenched into one of the many possible metastable configurations. It is therefore not surprising that inside the coexistence region  $\Delta P_W$  and  $\Delta P_C$  are different.

The coexistence boundary shown in Fig. 1 is essentially a plot of  $T_b$ , as given by the dissipation and history dependent  $\Delta P$  results for samples of different  $X_3$ . The boundary resembles that of the bulk mixture for  $X_3 \leq 0.5$  but indicates the presence of a miscible, superfluid mixture at high  $^3\text{He}$  concentrations. In the  $T=0$  K limit, the

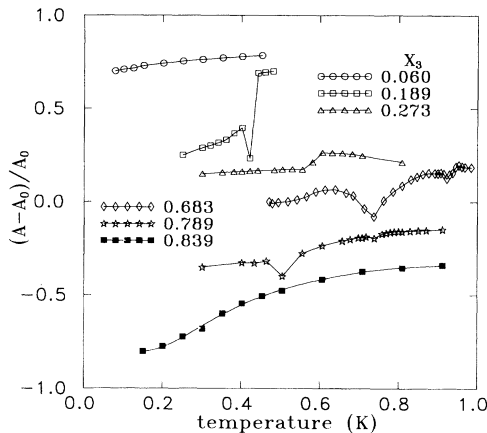


FIG. 5. Amplitude of oscillation as a function of temperature.  $A$  is the amplitude at temperature  $T$ ;  $A_0$  is the amplitude at the lowest temperature for each of the scans shown. All scans, except that at  $X_3=0.683$ , are shifted vertically for clarity. Dips and steps at intermediate  $X_3$  are interpreted as features related to the crossing of the coexistence boundary. Smaller dips at higher temperatures for mixtures at  $X_3=0.789$  and  $0.683$  are related to superfluid transitions. The scan at  $X_3=0.06$  is characteristic of scans at lower  $X_3$  and the scan at  $X_3=0.839$  is characteristic of those at  $X_3 \geq 0.839$ . These scans show no sign of crossing the coexistence boundary.

high  $X_3$  miscible superfluid is found between  $X_3=0.81$  and  $X_3=0.967$ . At intermediate concentrations, it shows a bump protruding to higher temperatures and terminating at a critical point near  $T=0.85$  K and  $X_3=0.57$ . We do not have an explanation for this protrusion near the critical point except to speculate that this may be related to critical fluctuations in the mixture.

The Blume-Emery-Griffiths (BEG) model [8] has been shown to be quite successful in describing the behavior of the  $^3\text{He}$ - $^4\text{He}$  mixture near the tricritical point. A recent calculation [9] mimics the effect of aerogel on the mixture as quenched randomness in the anisotropy parameter in the BEG model. Within such a framework, the tricritical point was found to be unstable and can lead to a phase diagram at least near  $T=T_{tr}$  similar to that found in this experiment.

Our interpretation of the findings near  $T=0$  are as follows: At low  $^4\text{He}$  concentrations, the  $^4\text{He}$  atoms are "plated" out of the mixture and become strongly bound onto the walls of the silica strands forming a solidlike, localized  $^4\text{He}$  layer, similar to that found in experiments of adsorbed  $^4\text{He}$  films [10]. A nearly pure  $^3\text{He}$  fluid is left surrounding the  $^4\text{He}$  coated silica strands. After the completion of the localized layer, additional  $^4\text{He}$  atoms are dissolved in the fluid, forming a miscible  $^3\text{He}$  rich solution which displays superfluidity at sufficiently low temperature. This occurs when the  $^4\text{He}$  concentration exceeds 3.3%. Because of the zero point energy and van der Waals interaction considerations mentioned above, one would expect the  $^4\text{He}$  atoms, even in this miscible fluid region, to accumulate preferentially near the (localized layer coated) silica strands. There is, however, no well-defined interface separating the  $^4\text{He}$  and  $^3\text{He}$  rich phases. Only when the average  $^4\text{He}$  concentration exceeds 19% does the mixture begin to phase separate into  $^4\text{He}$  rich and  $^3\text{He}$  rich regions.

At this point we do not have a quantitative model on why aerogel (in contrast to planar substrates [11,12]) is effective in suppressing phase separation at high  $X_3$ . It is likely to be related to the unique microstructure of the silica network in aerogels. Based on surface area ( $580 \text{ m}^2/\text{g}$ ) and density ( $0.044 \text{ g/cm}^3$ ) information of our aerogel sample, the silica network in aerogel can be modeled as strands of roughly  $31 \text{ \AA}$  in diameter. In the event of phase separation, the interface would be a cylindrical surface enclosing the  $^4\text{He}$  rich phase. For a mixture of low  $^4\text{He}$  concentration, it is costly to form such an interface of very small radius of curvature. The fact that phase separation at low  $^4\text{He}$  concentration is suppressed indicates that the energy gained by placing  $^4\text{He}$  atoms together is not sufficient to compensate the cost in forming such an interface.

One might argue instead that there is no miscible mixture of high  $^3\text{He}$  concentration, and the superfluid signal shown in Fig. 2 is due to a phase separated  $^4\text{He}$  film on silica strands that thickens with the addition of  $^4\text{He}$  atoms. To check this possibility, we repeated the mea-

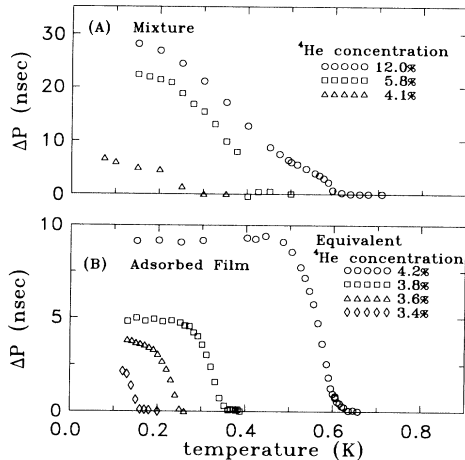


FIG. 6.  $\Delta P$  vs temperature for mixtures from (a) Fig. 2 and (b) thin  $^4\text{He}$  films adsorbed in the same aerogel torsional cell. For easy comparison,  $\Delta P$  values for mixture with 12%  $^4\text{He}$  have been multiplied by 0.2. See text for the meaning of equivalent  $^4\text{He}$  concentrations. The minimum (localized layer) film coverage needed for superfluidity in adsorbed films is  $36 \mu\text{mole/m}^2$ , corresponding to an equivalent  $^4\text{He}$  concentration of 3.1%. The minimum  $^4\text{He}$  concentration needed for superfluidity in mixtures is  $(3.3 \pm 0.2)\%$ .

measurements by first removing the mixture from the cell and dosing in an amount of  $^4\text{He}$  (to form an adsorbed film) that corresponds to that contained in a mixture with a few percent of  $^4\text{He}$ . For easy comparison, the  $^4\text{He}$  film coverage is expressed as "equivalent"  $^4\text{He}$  concentration in Fig. 6(b). This equivalent  $^4\text{He}$  concentration would be the concentration of a mixture if the remaining open volume in aerogel is filled with  $^3\text{He}$ . The superfluid properties (e.g., the temperature dependence of  $\Delta P$ ) of the mixtures [Fig. 6(a)] are completely different from that of the adsorbed films [Fig. 6(b)]. For adsorbed films, both  $\Delta P(0)$ , the superfluid signal at  $T=0$  (obtained via extrapolation) and  $T_c$  increase linearly with  $^4\text{He}$  coverages beyond the localized layer coverages. These linear dependences are not seen for mixtures. On a planar substrate, on the other hand, the superfluid properties of a phase separated  $^4\text{He}$  film sandwiched between the substrate and twelve layers of  $^3\text{He}$  resemble that of a pure  $^4\text{He}$  film exhibiting Kosterlitz-Thouless-like behavior. The only effect of the overburden of twelve layers of  $^3\text{He}$  is to require an additional one-half layer of  $^4\text{He}$  before superfluidity can occur [12]. These comparisons appear to confirm our interpretation of a miscible (albeit with concentration gradient) superfluid at high  $X_3$ . In other

words,  $^4\text{He}$  atoms dissolved in the mixture are responsible for the observed superfluidity at high, as well as low,  $^3\text{He}$  concentrations. If this picture is correct,  $^4\text{He}$  atoms in the high  $X_3$  limit may be considered as dilute Bose particles. If this mixture is cooled down to 1 mK, there is also the likelihood of finding an interpenetrating double superfluid. Experiments are in progress to check these fascinating possibilities.

We are indebted to Dr. L. W. Hrubesh of the Lawrence Livermore National Laboratory for growing the aerogel. We acknowledge useful conversations with G. Agnolet, P. W. Anderson, J. R. Banavar, M. W. Cole, D. O. Edwards, D. S. Fisher, M. E. Fisher, A. Maritan, and H. Meyer. This work is supported by NSF under Grants No. DMR-9008461 and No. DMR-9311918.

\*Present address: Department of Physics, Amherst College, Amherst, MA 01002.

- [1] E. H. Graf, D. M. Lee, and J. D. Reppy, Phys. Rev. Lett. **19**, 417 (1967).
- [2] E. M. Ifft, D. O. Edwards, R. J. Sarwinski, and M. M. Skertic, Phys. Rev. Lett. **19**, 831 (1967); C. Ebner and D. O. Edwards, Phys. Rep. **2C**, 77 (1970).
- [3] *Aerogels*, edited by J. Fricke (Springer-Verlag, Berlin, 1986); J. Fricke, Sci. Am. **258**, No. 5, 92 (1988).
- [4] T. M. Tillotson, L. W. Hrubesh, and I. M. Thomas, Mater. Res. Soc. Symp. Proc. **121**, 685 (1988).
- [5] J. Ma, A. P. Y. Wong, L. W. Hrubesh, and M. H. W. Chan (to be published).
- [6] Ray Radebaugh, *Thermodynamics Properties of  $^3\text{He}$ - $^4\text{He}$  Solution*, NBS Technical Note No. 342 (U.S. Dept. of Commerce, Washington, D.C., 1967).
- [7] D. M. Lee and H. A. Fairbank, J. Phys. Fluids **2**, 5 (1959); D. M. Lee, H. A. Fairbank, and E. J. Walker, Phys. Rev. **121**, 1258 (1961); C. Boghosian, H. Meyer, and J. E. Rives, Phys. Rev. **146**, 110 (1966).
- [8] M. Blume, V. J. Emery, and R. B. Griffiths, Phys. Rev. A **4**, 1071 (1971).
- [9] A. Maritan, M. Cieplak, M. Swift, F. Toigo, and J. R. Banavar, Phys. Rev. Lett. **69**, 221 (1992).
- [10] See, for example, G. Agnolet, D. F. McQueeney, and J. D. Reppy, Phys. Rev. B **39**, 8934 (1983); B. C. Crooker, B. Hebral, E. N. Smith, Y. Takano, and J. D. Reppy, Phys. Rev. Lett. **51**, 666 (1983); D. Finotello, K. A. Gillis, A. Wong, and M. H. W. Chan, Phys. Rev. Lett. **61**, 1954 (1988).
- [11] J. P. Romagnan, J. P. Laheurte, J. C. Noiray, and W. F. Saam, J. Low Temp. Phys. **70**, 425 (1978); F. M. Ellis, R. B. Hallock, M. D. Miller, and R. A. Guyer, Phys. Rev. Lett. **46**, 1461 (1981).
- [12] D. McQueeney, G. Agnolet, and J. D. Reppy, Phys. Rev. Lett. **52**, 1325 (1984).